Preliminary multi-axial strain analysis in wind turbine blades under fatigue test loads

Castro, Oscar; Branner, Kim

Published in:
I O P Conference Series: Materials Science and Engineering

Link to article, DOI:
10.1088/1757-899X/942/1/012044

Publication date:
2020

Document Version
Publisher's PDF, also known as Version of record

Preliminary multi-axial strain analysis in wind turbine blades under fatigue test loads

IOP Conf. Series: Materials Science and Engineering **942** (2020) 012044 doi:10.1088/1757-899X/942/1/012044

Preliminary multi-axial strain analysis in wind turbine blades under fatigue test loads

Oscar Castro and Kim Branner
Technical University of Denmark, DTU Wind Energy, Frederiksborgvej 399, 4000 Roskilde
E-mail: osar@dtu.dk and kibr@dtu.dk

Abstract. A preliminary experimental characterization of the longitudinal, transverse, and shear strains in wind turbine blades under fatigue loading is presented in this study. For that, strains at different cross-section regions of a 14.3 m blade under different uni-axial and biaxial fatigue tests are recorded and analyzed. The results from this analysis provide initial indications on how current testing methods used to certify and characterize the fatigue response of wind turbine blade materials can be improved to better represent what the blades experience during testing. It is shown, for example, how some of the blade regions can experience high biaxiality strain ratios, and how some of these regions can also experience broad internal loading conditions, in terms of strain levels and load orientation (i.e., compression, tension-compression, and tension), depending on the test type.

1. Introduction

Different testing methods are currently used to certify and characterize the fatigue response of wind turbine blades and their materials, which are mainly carried out at the full-length scale [1, 2] and at the coupon-length scale [3, 4]. However, there are various reasons that motivate us to question how representative these methods are. For example, are the loads applied during the coupon-scale fatigue tests representing the internal material loads of the blade during full-scale fatigue tests? In this paper, we will contribute to the discussion of this question.

At the full-length scale, only one or two blades are normally tested according to the standards [1, 2]. In these tests, the blades are commonly evaluated consecutively under flapwise and edgewise fatigue loading, although these structures are subjected to combined loads in real operational conditions [5, 6]. In addition, target bending moments in the flapwise and edgewise directions are usually used alone to design the certification tests, which may disregard the actual effects of the loads on the material response [6].

At the coupon-length scale, on the other hand, 8-10 specimens are commonly used to obtain one S-N curve for a given R-ratio (i.e., the ratio between the minimum and maximum cyclic stress, $R = \sigma_{min}/\sigma_{max}$.) and material orientation, θ, [4]. This is normally done for $\theta = 0°$ and $R = 0.1$ and, occasionally, also for $R = -1.0$ and/or $R = 10.0$. Sometimes, $\theta = 90°$ is also considered. In this way, in the best scenario, the fatigue behavior of the material in the longitudinal and transverse directions under specific R-ratios is characterized. Moreover, these tests are carried out by applying uni-axial loading to the specimens [4], which may ignore the effects of external biaxial loading conditions generally presented in wind turbine blades [5].

Some studies have attempted to assess the blade response during fatigue testing at the material level by considering strains [5] and strain-based damage targets [7] instead of only

bending-moment-based damage targets. In that way, a better connection between the full-length scale and the coupon-length scale could be achieved. Nevertheless, such approaches only consider the strains in the longitudinal blade direction omitting, therefore, possible effects of transverse and shear strains that might be significant in some of the materials used in wind turbine blades, such as composite materials [8].

Little attention has been given to quantifying the multi-axial strain/stress levels and local load orientation (i.e., compression, tension-compression, and tension) in wind turbine blades under uni-axial and biaxial loading conditions, which could contribute to making a better connection between the fatigue tests at the different length scales. In [9], the estimated fatigue effects of variable wind load and non-proportional multi-axial stress states in a wind turbine blade were studied. However, the results were given by means of an equivalent multi-axial fatigue damage index, which makes difficult to quantify the multi-axial strain levels and the local load orientation in the blade.

In this sense, this study presents a preliminary quantification of the multi-axial strain distribution in wind turbine blades under full-scale testing loads. Initial measurements of longitudinal, transverse, and shear strains in different blade regions and under different loading conditions are reported and analyzed in terms of multi-axial strain levels and local load orientation. The results of this study are expected to contribute to making the fatigue coupon-length scale tests more representative respect to the fatigue full-length scale tests.

2. Methods

A commercial 14.3 m wind turbine blade [7] is used in this study. This blade type has been intensely tested at DTU Large Scale Facility, LSF, of the Wind Energy Department, Technical University of Denmark. Longitudinal, transverse, and shear strains ($\epsilon_{amp,x}$, $\epsilon_{amp,y}$, and $\epsilon_{amp,xy}$, respectively), were measured by using strain gauge rosettes installed on the outer surface of the blade, see Fig. 1. The longitudinal measurements were aligned with the global longitudinal blade direction. The strains were measured at the trailing-edge (TE), trailing-edge panel (TE-Panel), spar-cap (Cap), and leading-edge (LE1 and LE2) regions of the suction side of cross-sections located at 3.35 m and 7.8 m from the root, see Fig. 1 and Table 1. Measurements were done over 600 s for each load case, with sampling frequency of 100 Hz. Afterwards, the Gaussian method [10] was used to clean the noise from the data.

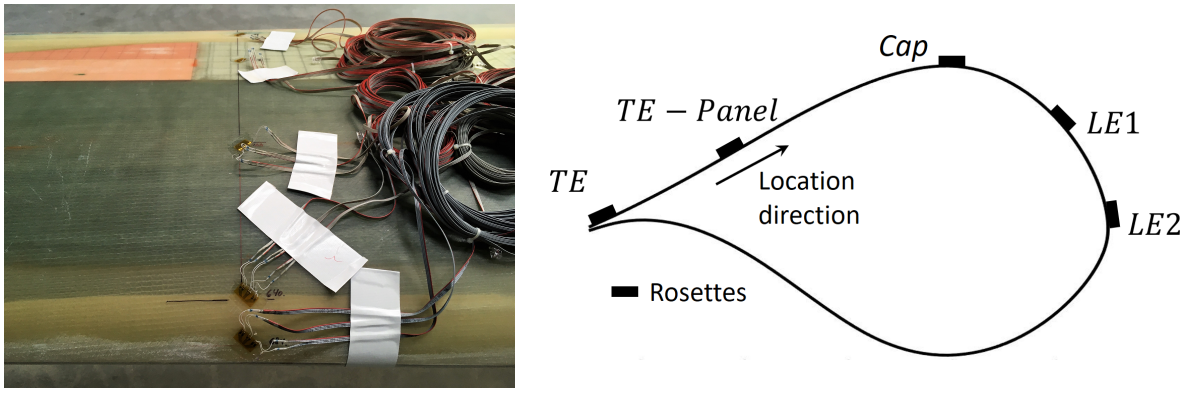

Figure 1. Strain gauge rosette locations on the blade surface.

These measurements were obtained under different loading conditions, including two flapwise loads (Flap-01 and Flap-02), two edgewise loads (Edge-01 and Edge-02), and three chaotic loads (Chao-01, Chao-02, and Chao-03). The loads were applied to the blade by using a ground-based resonance exciter located at 5.2 m from the root. More details about the test setup and loading

Table 1. Strain gauge rosette locations on the suction-side surface, measured from the trailing-edge towards the leading-edge. Values in mm.

Cross-section location [m]	TE	TE-Panel	Cap	LE1	LE2
3.35	20	323	782	1141	1281
7.80	20	165	441	640	684

conditions are shown in Table 2. In addition, an explanation of chaotic loading can be found in [5, 7].

Table 2. Forces, F, applied to the blade in the flapwise and edgewise directions for the different evaluated load cases. The flapwise frequency, f_{flap}, and edgewise frequency, f_{edge}, for all cases were 2.315Hz and 4.595Hz, respectively.

Load case	F_{flap} [kN]	F_{edge} [kN]	Load case	F_{flap} [kN]	F_{edge} [kN]
Flap-01	2.00	-	Flap-02	3.00	-
Edge-01	-	0.50	Edge-02	-	0.75
Chao-01	2.00	0.50	Chao-02	3.00	0.50
Chao-03	2.00	0.75	-	-	-

The different strain time series at the cross-section regions were reduced into a number of constant-amplitude strain-cycle blocks by using the rainflow counting method [11]. Each of these blocks were characterized using the Q-ratio (i.e., $Q = \epsilon_{mean}/(\epsilon_{amp} - \mid \epsilon_{mean} \mid)$, where ϵ_{mean} is the mean strain and ϵ_{amp} is the strain amplitude [12]), as an alternative of the R-ratio. With the Q-ratio, all possible load conditions can be included continuously into a range from -1 to 1. This means that, for compression-compression (C-C), $-1.0 \leq Q < -0.5$; for compression-tension (C-T), $-0.5 \leq Q < 0$; for tension-compression (T-C), $0 \leq Q < 0.5$; and for tension-tension (T-T), $0.5 \leq Q < 1.0$.

3. Results and Discussion

In this section, the results and an analysis on the characterization of the multi-axial strain cycles at the different regions of the blade, under different types of load, are presented. The results of the LE1 region are not graphically shown in the paper as they were found to be similar than the ones obtained from the LE2 region. These similarities are due to the fact that both regions were made of the same material and layup, and that the measuring points were relatively close to each other.

The percentage of number of cycles, N/N_{total}, for a given Q-ratio and strain level, $\epsilon_{amp,i}/\epsilon_{amp,x,max}$, for different cross-section regions and under flapwise, edgewise, and chaotic loading conditions are presented in Figs. 2, 3, and 5, respectively. Where, $\epsilon_{amp,x,max}$ is the maximum strain amplitude in the longitudinal direction, N is the actual number of cycles under a given Q-ratio and $\epsilon_{amp,i}$; N_{total} is the total number of cycles within the time series; and $i = x$, y, or xy, denoting the longitudinal, transverse and shear directions, respectively.

As seen in Fig. 2, when a flapwise test is carried out, all cycles from the different strain components and at the different cross-sections regions are under C-T or T-C. In fact, most of them tend to a Q-ratio equal to zero, which would be equivalent to $R = -1.0$. This is because,

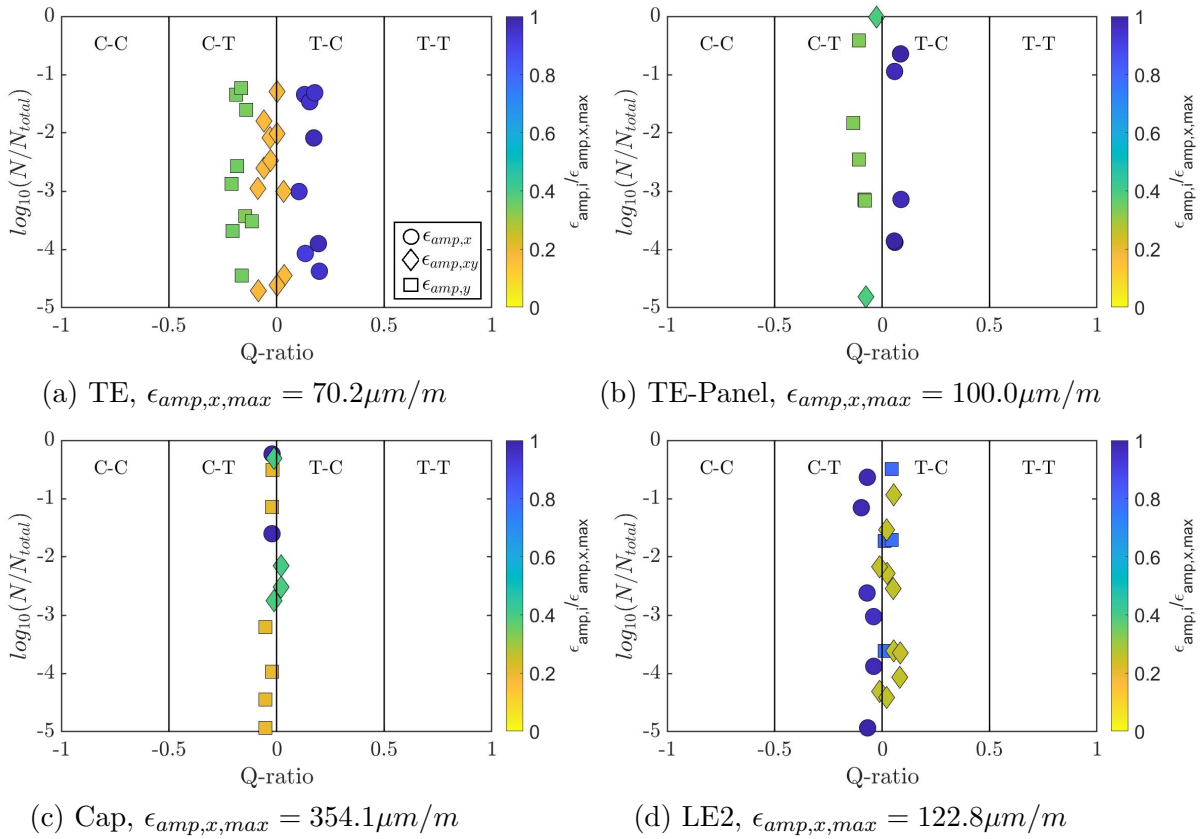

(a) TE, $\epsilon_{amp,x,max} = 70.2\mu m/m$

(b) TE-Panel, $\epsilon_{amp,x,max} = 100.0\mu m/m$

(c) Cap, $\epsilon_{amp,x,max} = 354.1\mu m/m$

(d) LE2, $\epsilon_{amp,x,max} = 122.8\mu m/m$

Figure 2. $N/N_{total} - Q - \epsilon_{amp,i}/\epsilon_{amp,x,max}$ matrix of different cross-section regions: (a) TE, (b) TE-Panel, (c) Cap, and (d) LE2, at 3.35m span. Flap-02 test case.

during the test, the load applied by the exciter also has a $Q = 0$, meaning that the maximum and minimum applied load have the same value but with opposite signs. Moreover, although the load is applied in the global flapwise direction (i.e., with respect to the root-coordinate system), a small load component in the edgewise direction is also presented in the local cross-section-coordinates due to the orientation of the local principal axes. This can be seen as the TE and LE experience some deformations as well, see Figs. 2-a and 2-d, respectively.

Similarly, when an edgewise test is carried out, most of cycles from the different strain components and at the different cross-sections regions are under C-T or T-C loading conditions, see Fig. 3. This except for some transverse and shear strain cycles at the Cap region, which were under T-T and C-C, see Fig. 3-c. These cycles can be related to noise in the signal as the strain amplitudes in these two directions were low and noisy, see Fig. 4, and the data was not properly cleaned. Omitting this noise, it can be seen that the strain amplitude in the transverse direction was almost zero (i.e., $Q = -1.0$), whereas the main strain components in the shear direction had a Q-ratio close to 0.35.

It is worth to note that, for the flapwise and edgewise tests, the strain time series for the different strain components and at the different cross-section regions can be simplified as a few constant-amplitude blocks with similar strain level and Q-ratio, see Figs. 2 and 3. This is because the load is applied in only one direction and the frequency with which it is applied remains, in theory, constant during the test.

However, when a chaotic test is carried out, several block cycles with a bigger difference in the strain level and Q-ratio define the different strain time series for the different strain

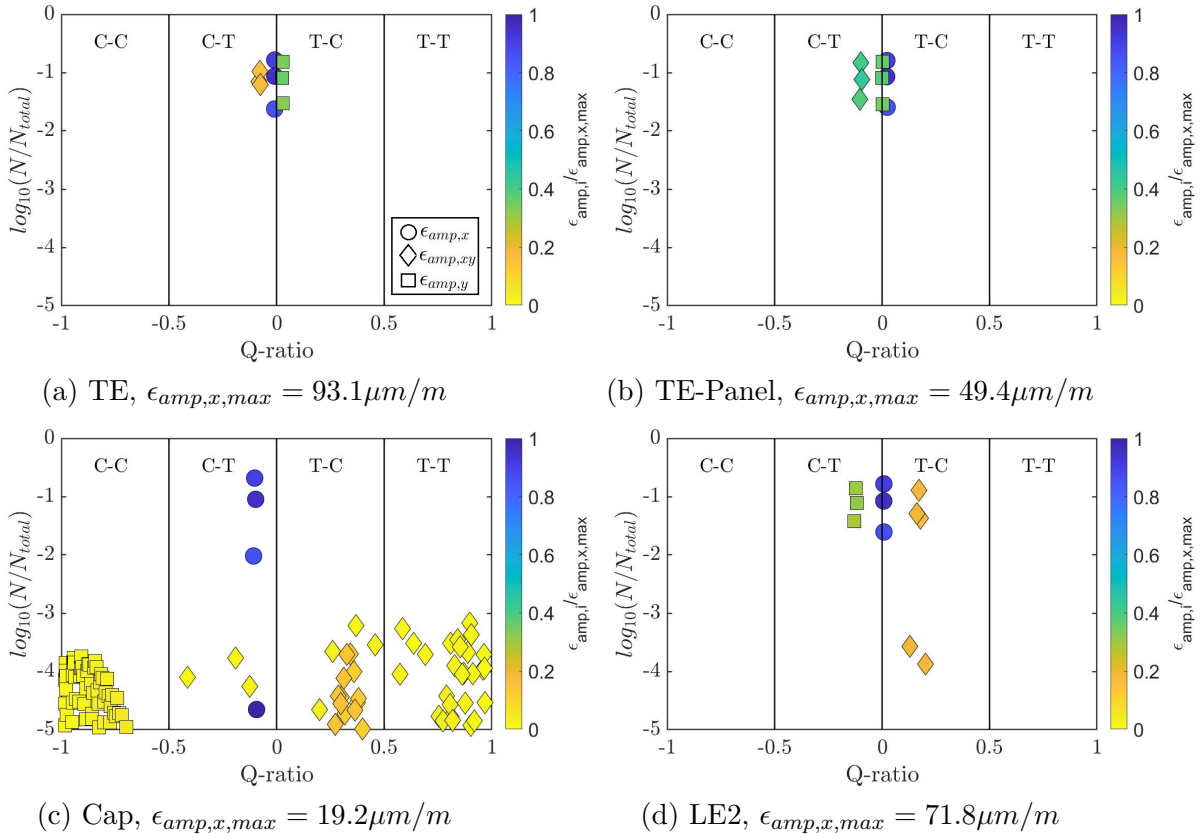

(a) TE, $\epsilon_{amp,x,max} = 93.1\mu m/m$

(b) TE-Panel, $\epsilon_{amp,x,max} = 49.4\mu m/m$

(c) Cap, $\epsilon_{amp,x,max} = 19.2\mu m/m$

(d) LE2, $\epsilon_{amp,x,max} = 71.8\mu m/m$

Figure 3. $N/N_{total} - Q - \epsilon_{amp,i}/\epsilon_{amp,x,max}$ matrix of different cross-section regions: (a) TE, (b) TE-Panel, (c) Cap, and (d) LE2, at 3.35m span. Edge-01 test case.

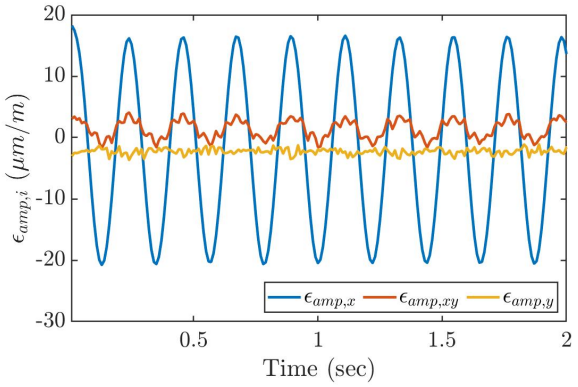

Figure 4. Strain time series at the Cap region for the Edge-01 test case. Note the noisy signals for $\epsilon_{amp,xy}$ and $\epsilon_{amp,y}$.

components, see Fig. 5. This is because, during the chaotic tests, the flapwise and edgewise forces have different frequencies, and both the magnitude of each of them and the phase angle between them change with time, which causes strains to change significantly over time, see Fig. 6. Moreover, as seen in Fig. 5, most of the cycles from the different strain components and at the different cross-section regions are under C-T and T-C, except for some cycles with low strain level that are under C-C and T-T, see Fig. 5-d. In this case, these cycles are not necessarily related to noise in the signal as in the edgewise-test case. In fact, they do exist as a consequence of the superposition of the two external forces, see e.g. in Fig. 6.

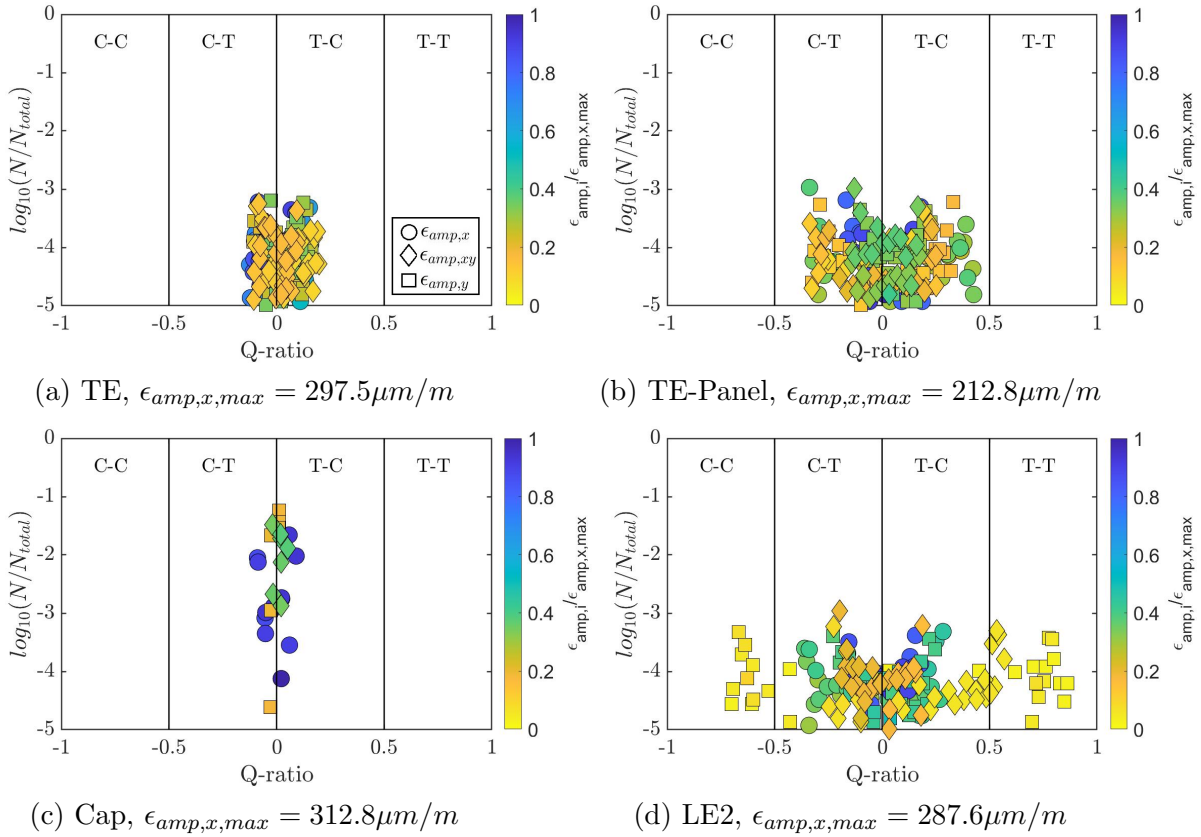

(a) TE, $\epsilon_{amp,x,max} = 297.5\mu m/m$ (b) TE-Panel, $\epsilon_{amp,x,max} = 212.8\mu m/m$

(c) Cap, $\epsilon_{amp,x,max} = 312.8\mu m/m$ (d) LE2, $\epsilon_{amp,x,max} = 287.6\mu m/m$

Figure 5. $N/N_{total} - Q - \epsilon_{amp,i}/\epsilon_{amp,x,max}$ matrix of different cross-section regions: (a) TE, (b) TE-Panel, (c) Cap, and (d) LE2, at 3.35m span. Chao-02 test case.

On the other hand, it was found that, although the longitudinal strains are the dominant strain component in the blade, the transverse and shear strain components can also have significant magnitudes in some of the cross-section regions, see e.g. in Fig. 2, 3, and 5. In general, for the shear strains, significant magnitudes (i.e., $\epsilon_{amp,xy}/\epsilon_{amp,x,max} \geq 0.4$) were found at the TE-Panel for all test cases, and at the Cap for the flapwise and chaotic test cases. Whereas, for the transverse strains, significant magnitudes (i.e., $\epsilon_{amp,y}/\epsilon_{amp,x,max} \geq 0.4$) were found at the TE, TE-Panel, and LE2 regions, for all test cases.

Moreover, for each cross-section, there was not a considerable qualitatively difference between the strain behavior at the different cross-section regions with the variation of the load level, see e.g. in Figs. 7-a and 7-b, and 7-c and 7-d, respectively. The variation was mainly quantitatively, as the strains increase with the increase of the load. In addition, for a given load level applied to the blade, some qualitatively and quantitatively differences can occur between the different cross-sections, see e.g. in Figs. 7-a and 7-c, and 7-b and 7-d, respectively. This is because the cross-section geometry, the cross-section properties, and the loads, among other factors, change along the blade span.

All this suggests that, a more comprehensive fatigue characterization at the coupon-length scale level might be needed to better predict the material response due to the loads that the blades experience when subjected to more realistic loading conditions, such as chaotic loads. In addition, the consideration of the transverse and shear strain components might be relevant for most of the cross-section regions, specially at the TE-Panel.

A similar study to this one, in which the actual operational loads that the blades experience

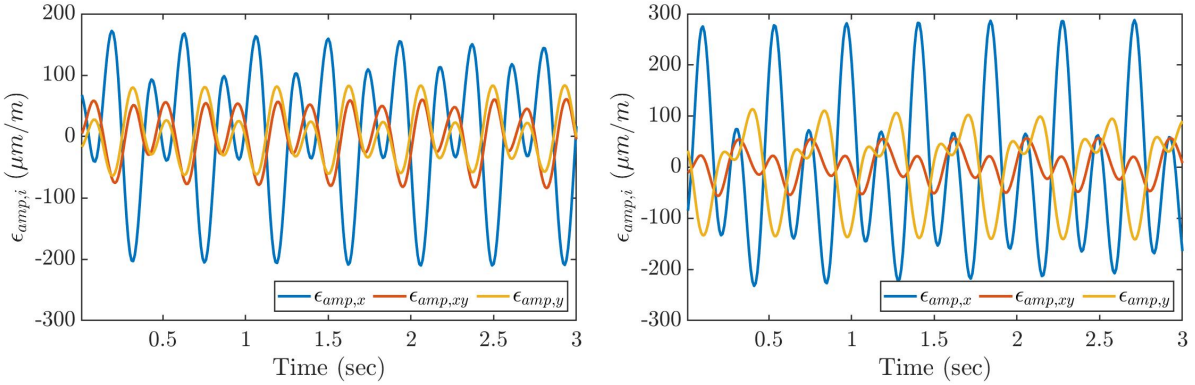

(a) TE-Panel (b) LE2

Figure 6. Strain time series at different cross-section regions: (a) TE-Panel; and (b) LE2, at 3.35m span. Chao-02 test case.

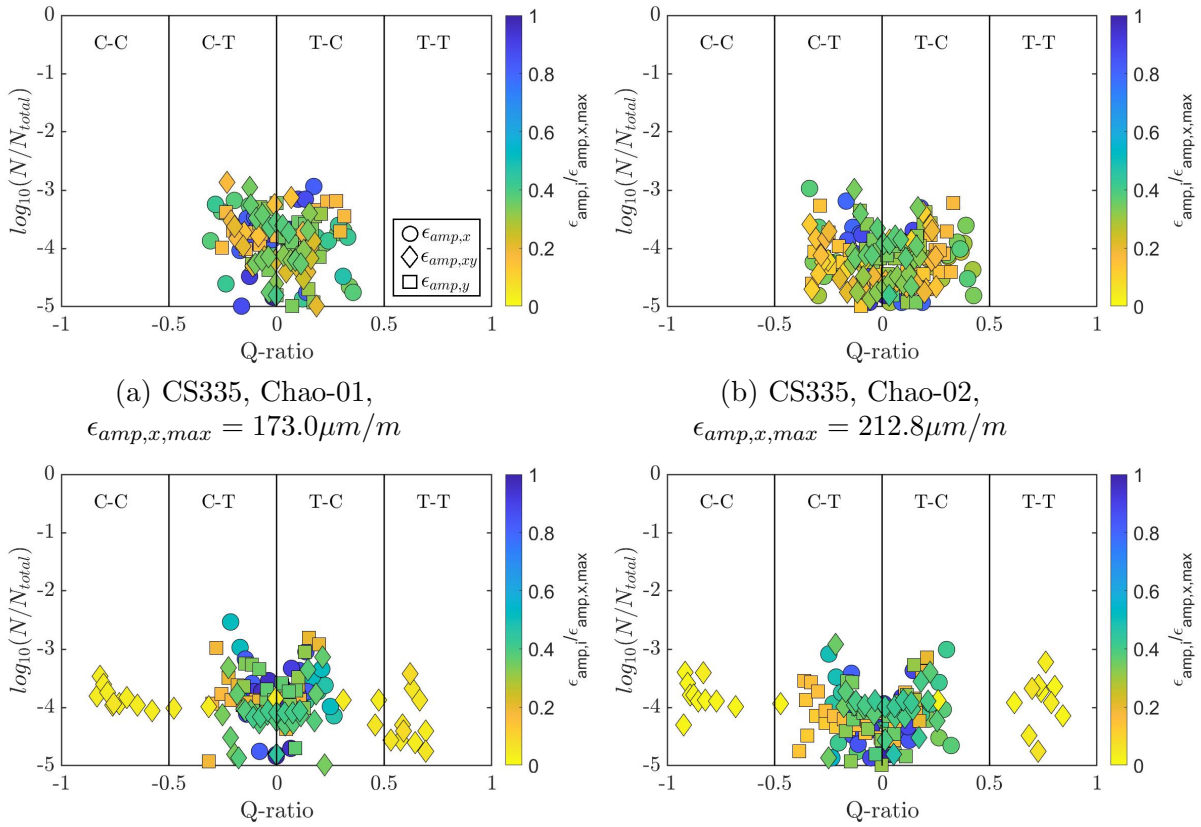

(a) CS335, Chao-01, $\epsilon_{amp,x,max} = 173.0\mu m/m$

(b) CS335, Chao-02, $\epsilon_{amp,x,max} = 212.8\mu m/m$

(c) CS780, Chao-01, $\epsilon_{amp,x,max} = 348.6\mu m/m$

(d) CS780, Chao-02, $\epsilon_{amp,x,max} = 430.9\mu m/m$

Figure 7. $N/N_{total} - R - \epsilon_{amp,i}/\epsilon_{amp,x,max}$ matrix of the TE-Panel under chaotic loading. At 3.35m span, (a) Chao-01 and (b) Chao-02. At 7.8m span, (c) Chao-01 and (d) Chao-02.

during their lifetime are considered, would provide a better indication of how well current fatigue tests methods at the different length scales represent reality. Furthermore, it would be also good to quantify the local strain behaviour at each of the layers within the different cross-section

regions (i.e., not only at the surface), as damages can develop at any layer. Moreover, it might be also necessary to quantify the interaction between the different strain components.

4. Conclusion

A preliminary experimental characterization of the longitudinal, transverse, and shear strain cycles at different regions of a 14.3 m blade under different uni-axial and biaxial fatigue test loading conditions, was presented in this paper. Under uni-axial loading, the time series from all strain components and at all evaluated cross-section regions could be simplified as a few blocks of cycles with similar Q-ratio and strain levels, being most of them under C-T and T-C. Whereas, under chaotic loading, the time series from all strain components were composed by a larger number of block cycles under C-T and T-C and with broader Q-ratio and strain levels. Some of the strain block cycles at the leading-edge were also under T-T and C-C. Furthermore, it was also found that the transverse and shear strain components can have a significant magnitude in most of the cross-sections regions, specially at the TE-Panel, if compared with the respective longitudinal strains (i.e., more than 40% of the longitudinal strains). Hence, this work provides initial indications about how current certification fatigue test methods for wind turbine blade materials can be improved in order to account for the biaxiality ratio between the different strain components and the broad internal loading conditions (i.e., T-T, C-C, T-C, and C-T) that the different blade cross-section regions can undergo, specially under external biaxial loading.

Acknowledgments

The work is supported by the Danish Energy Agency through the Energy Technology Development and Demonstration Program (EUDP), Grant No. 64016-0023. The supported project is named "BLATIGUE: Fast and efficient fatigue test of large wind turbine blade." The financial support is greatly appreciated. The authors would also like to thank the technicians and engineers from the LSF, who contributed to setting up the blade and test.

References

[1] IEC-61400-23 2014 Wind turbines – part 23: Full-scale structural testing of rotor blades Standard International Electrotechnical Commission
[2] DNVGL-ST-0376 2015 Rotor blades for wind turbines Standard DNV-GL
[3] ISO-527-5 2009 Determination of tensile properties - part 5: Test conditions for unidirectional fibre-reinforced plastic composites Standard International Organisation for Standardization (ISO)
[4] ISO-13003 2003 Fibre reinforced plastics – determination of fatigue properties under cyclic loading conditions Standard International Organisation for Standardization (ISO)
[5] Greaves P 2013 *Fatigue analysis and testing of wind turbine blades* Ph.D. thesis Durham University Durham (Eng)
[6] Hughes S D, Musial W D and Stensland T 1999 Implementation of a two-axis servo-hydraulic system for full-scale fatigue testing of wind turbine blades Technical Report NREL/CP-500-26896 National Renewable Energy Laboratory Golden (CO)
[7] Castro O, Belloni F, Stolpe M, Yeniceli S C, Berring P and Branner K 2020 *Optimized method for multi-axial fatigue testing of wind turbine blades. Compos Struct (submitted for publication)* xx–xx
[8] Quaresimin M, Susmel L and Talreja R 2010 *Int J Fatigue* **32** 2 – 16
[9] Hu W, Zhupanska O, Choi K and Buchholz J 2015 *Proceedings of the American Society for Composites 30th Technical Conference, 2015* (American Society for Composites)
[10] Haddad R A and Akansu A N 1991 *IEEE Transactions on Signal Processing* **39** 723–727
[11] ASTM-E1049-85 2017 Standard practices for cycle counting in fatigue analysis Standard ASTM International
[12] Westphal T 2012-10-08 Personal communication